Pol. J. Environ. Stud. Vol. XX, No. X (XXXX), 1-16
DOI: 10.15244/pjoes/195364 ONLINE PUBLICATION DATE:

Original Research

Evaluating Spatiotemporal Patterns of Non-Point Source Pollution and Related Mitigation Measures in High Density Urban Area Using the SWAT Model

Aobo Sun*

School of Future Technology, South China University of Technology, Guangzhou City Guangdong Province, 510641, China

Received: 9 August 2024
Accepted: 28 October 2024

Abstract

With the enhancement of sewage and drainage system infrastructure and the increase in water quality purification plant effluent standards in urban regions of China, point-source pollution in most urban areas has been effectively controlled. However, due to the rapid population growth and expansion of urban areas during the urbanization process, non-point source pollution plays an increasingly important role in the pollution of urban surface water. This study addresses the existing challenges in accurately quantifying loads and identifying characteristics of non-point source pollution in high density urban areas by taking the Guanlan River basin as a case study area. The Soil and Water Assessment Tool (SWAT) model was used to simulate the total nitrogen (TN) and total phosphorus (TP) loads originating from non-point source pollution in the basin, as well as to identify their spatiotemporal patterns. Through establishing two pollution mitigation measures comprising six scenarios, in conjunction with the SWAT model, the mitigated efficiency of TN and TP levels for each scenario in the case study area in 2022 was evaluated. The simulated values of the SWAT model revealed a good agreement with the observed data for runoff, TN, and TP. The SWAT model was employed to examine spatiotemporal characteristics of non-point source pollution TN and TP loads in the study area in 2022. Spatially, some sub-basins exhibited relatively high levels, with TN levels varying between 1036.1 and 1523.9 kg/km^2 and TP levels ranging from 473.5 to 572.9 kg/km^2. Temporally, the most severe precipitation runoff pollution was recorded in May, where TN and TP loads reached 252.47 kg/km^2 and 215.91 kg/km^2, respectively. It was observed that both filter strips and grassed waterways measures have been proven effective in mitigating non-point source pollution in the case study area. These engineering measures indicate the appealing potential in reducing the TN and TP from non-point source pollution in high density urban areas China-wide.

Keywords: high density urban area, non-point source pollution, SWAT, Guanlan River basin, mitigation measures

*e-mail: 202264690410@mail.scut.edu.cn

Introduction

Water is a critical natural resource that plays a fundamental role in the sustainability of all living organisms. Without access to clean and safe water, human beings would struggle to survive. With rapid socio-economic and urbanization development, the demand for water resources in human activities continues to escalate [1]. Concurrently, ecological issues manifest frequently and are related to severe water pollution challenges [2]. Effectively addressing water pollution has become a critical concern for policymakers [3]. A study conducted recently found that non-point source pollution exceeds point source pollution, emerging as a main concern for the quality of surface water, especially in China [4]. Non-point source pollution is a significant environmental issue that is often divided into two main categories: agricultural non-point source pollution and urban non-point source pollution [5]. Agricultural non-point source pollution refers to the contamination of water bodies from various sources, such as fertilizers, pesticides, and animal waste, that are not directly discharged into a waterway but rather carried by runoff. On the other hand, urban non-point source pollution stems from a variety of sources in urban areas, including stormwater runoff, road salts, and litter. Both types of non-point source pollution pose challenges for water quality management and require effective strategies to mitigate their impact on the environment. In recent years, significant advancements have been made in sewage and drainage system infrastructure [6]. These improvements, coupled with the elevation of effluent standards for water quality purification plants, have led to more effective management of point source pollution. As a result, in areas with high population density and extensive urban development, pollution originating from specific, identifiable sources has been progressively brought under control. However, with continued urbanization, the increased proportion of impermeable surfaces, intricate human activities, and diverse pollution sources exacerbate river pollution. The growing recognition of the effects of non-point source pollution on surface water quality in densely populated urban areas is becoming more evident. Thus, there is an urgent need to quantify the pollution load and specify the spatiotemporal characteristics of this pollution. This foundational knowledge is crucial for implementing effective management strategies aimed at mitigating the degradation of urban surface water quality. By adopting appropriate control measures, we can significantly enhance the water environment of urban rivers, contributing to healthier and more sustainable urban ecosystems.

Urban non-point source pollution consists mainly of nutrients like nitrogen and phosphorus, along with dissolved organic matter. Once generated and released, it infiltrates the water bodies through a series of transfer processes, such as effective rainfall and runoff transport [7]. Non-point source pollution is characterized by ambiguity, stochasticity, lagging, and hiddenness that are different from point source pollution, making the estimation and modeling of its pollution loads particularly challenging [8]. There are two main methods for estimating non-point source pollution loads: empirical estimation models and physically-based hydrological models. Empirical models rely on empirical formulas for estimation but may lack precision in load quantification [9]. In comparison, physically-based hydrological models fully consider the spatial heterogeneity within basins, providing a more detailed and accurate depiction of hydrological processes within the basin, and have been widely applied [10].

At present, non-point source pollution simulation models include the HSPF model (Hydrological Simulation Program - FORTRAN), the AGNPS model (Agricultural Non-Point Source Pollution Model), and the SWAT model [11]. Particularly, the SWAT model has attracted wide attention because of its open-source nature, robust physical mechanism, and distributed hydrological units [12-15]. The high-precision simulation capacity of this SWAT model allows for accurate modeling of non-point source pollution from agricultural activities in large watersheds [16]. Consequently, this capability has facilitated its widespread application on a global scale [17-19]. However, there is a lack of research on the quantification of urban non-point source pollution loads and the analysis of their impact effects in small-scale river basins within high density urban areas.

This study explores the non-point source pollution in the high density urban area of Shenzhen, one of the most densely populated, urbanized, and economically active cities in China. In particular, the focus of the study is on the Guanlan River Basin as the designated study area. Drawing from the monitoring data on flow and water quality at the basin's outlet, a SWAT model was meticulously established to analyze the non-point source pollution situation in the study area. The SWAT model parameters were adjusted to accurately represent the runoff and water quality within the watershed. This calibration and validation process ensured that the model's predictions were reliable and could be used to assess non-point source pollution in the area. By studying the spatial and temporal distribution of non-point source pollutants, researchers were able to acquire a more comprehensive insight into the influence of how urban surface water quality is impacted by various factors in the watershed. On this basis, two distinct non-point source pollution mitigation measures (three filter strip scenarios and three grassed waterways scenarios) were simulated to evaluate the efficiency and impact of each scenario in reducing non-point source pollution load. The measures proposed to mitigate non-point source TN and TP pollution in high density urban areas within the basin offer a solid foundation and practical assistance for effectively managing non-point source pollution in urban areas sharing similar basin characteristics. These strategies can serve as a model for other regions facing similar challenges, aiding

in the development and implementation of integrated management strategies to mitigate the impact of urban pollution on local surface water environments.

Materials and Methods

Study Area

The Guanlan River, a secondary tributary of the Dongjiang River basin in southern China, lows through the regions of Shenzhen and Dongguan [20]. This basin has a subtropical humid climate and is characterized by an average temperature of approximately 23°C (the maximum temperature in 2022 was 37.7°C and the minimum temperature was 5.5°C) for years and an average annual rainfall of around 1800 mm, most falling between April and September, with an annual average relative humidity of 76% and sunshine duration of 1850 h [21]. From 2015 to 2019, great efforts were made to enhance the surface water quality within the basin through the extensive construction of water pollution treatment facilities, such as pipelines and sewage treatment plants. Currently, the water quality monitoring site at the basin's outlet consistently meets the Class IV standard on average [22]. Despite these improvements, during rainy periods, the water quality often deteriorates to the Class V standard [22], resulting in challenges in maintaining stable water quality standards due to significant fluctuations. In the current situation of the study area, runoff pollution in high density urban areas stands out as the primary non-point source of pollution. This type of pollution occurs when rainfall water flows over these densely constructed areas, collecting various contaminants along the way. These pollutants can include substances such as oil, chemicals, and debris, which are then transported into water bodies, significantly affecting their quality [23]. Consequently, managing runoff pollution in these high density urban areas is crucial to controlling and mitigating non-point source pollution in the region. The basin area is about 256.72 km^2, and the current ground elevation of the area is 10-509 meters. The river water system of the study area is shown in Fig. 1.

SWAT Model

The SWAT model is a distributed hydrological model developed at the river basin scale by the United States Department of Agriculture Agricultural Research Service. It is designed to predict the impact of land management practices on water, sediment, and agricultural chemical yields within large and complex watersheds. This model accounts for varying soil types, land use, and management conditions over extended periods [24]. Additionally, it integrates Geographic Information System capabilities, leveraging spatial information obtained through remote sensing and

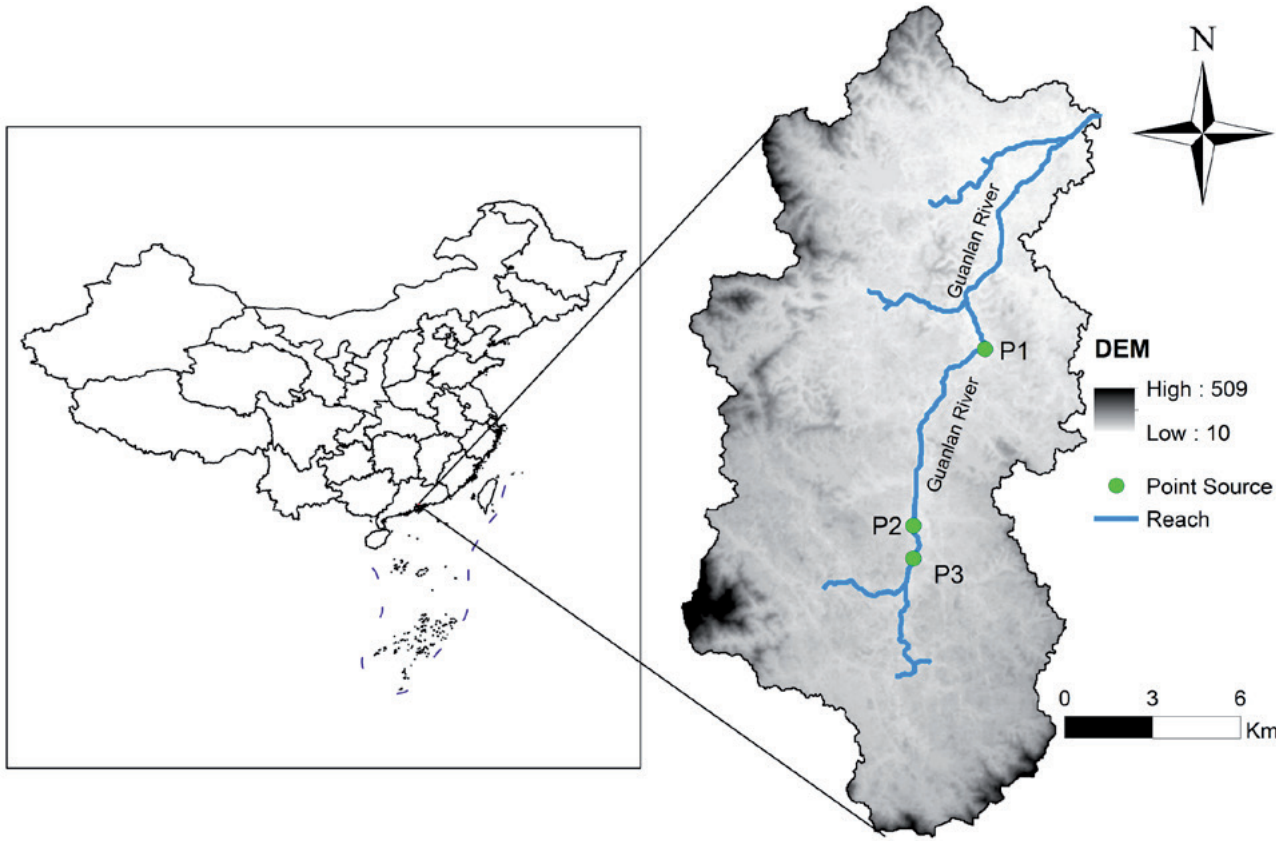

Fig. 1. The river water system of the study area.

geographic information systems alongside rainfall data to simulate and forecast the movement of nutrients, including runoff, nitrogen, and phosphorus, under different management scenarios.

Data

The SWAT model database primarily comprises spatial and non-spatial data components. Spatial data is utilized to identify the locations, while non-spatial data, known as attribute data, offers additional hydro-meteorological information. The digital elevation model (DEM) was obtained from the China Geospatial Data Cloud with a resolution of 30m, the land use type data was obtained from the Chinese Academy of Sciences with a resolution of 1km, the soil type data was obtained from the Harmonized World Soil Database with a resolution of 1km, the rainfall data was obtained from the Xiaogongyan Rainfall Station, and the meteorological data was obtained from the China Meteorological Data Network.

A relatively complete flow and water quality monitoring system has only been established in the study area since 2017, and the data obtained through long-term monitoring are critical for parameter calibration of the SWAT model. In addition, point source pollution collection and treatment facilities in the study area are inadequate until 2020, resulting in some point source pollution being discharged directly into the river, and this portion of the pollution load is difficult to quantify. After 2020, the main in-stream pollutants in the study area are non-point source pollution. Considering the availability of meteorological data, the simulation period for the established SWAT model is set as 2017-2022. Specifically, the period from 2017 to 2019 serves as the model's warm-up phase, 2020 to 2021 is set for calibration purposes, and 2022 is designated for validation. This approach improves the accuracy of the SWAT model simulations.

Discharge and Pollutant Concentration Restoration

Due to the implementation of waste-water treatment facilities along the Guanlan River's main stream within the study area, including the Guanlan waste-water treatment plant (P1 point in Fig. 1), Longhua waste-water treatment plant (P2 point in Fig. 1), and Banxuegang waste-water treatment plant (P3 point in Fig. 1), the combined designed treatment capacity amounts to 960,000 t/d. The production and domestic water in the Guanlan River basin come from cross-basin water diversion, which is discharged directly into the mainstream of the Guanlan River after being treated by the waste-water treatment plant, and the discharge standards of TN are less than 15 mg/L where TP is less than 0.5 mg/L.

To facilitate the assessment of the non-point source pollution load characteristics in the study area, based on the water quantity and quality monitoring data of the basin outlet in the study area, the water quantity and pollutants discharged from each waste-water treatment plant to the mainstream were deducted, and the discharge and pollutants related only to the non-point source pollution load were restored. The restored discharge can be expressed in formula (1).

$$Q_{m,i}=Q_{mt,i}-Q_{out,i} \tag{1}$$

where $Q_{m,i}$ represents the restored discharge, $Q_{mt,i}$ represents the measured discharge, $Q_{out,i}$ represents the tailwater discharge of the waste-water treatment plant, and i is the i^{th} measured interval, such as day or month.

The pollutant concentration can be calculated in formula (2).

$$C_{t,i}=\frac{Q_{mt,i}\times C_{mt,i}-Q_{out,i}\times C_{out,i}}{Q_{m,i}} \tag{2}$$

Where $C_{t,i}$ is the restored pollutant concentration, $C_{mt,i}$ is the measured pollutant concentration, $C_{out,i}$ is the pollutant concentration in the tailwater of the waste-water treatment plant.

Method of Calibration and Validation

For this research, the SUFI-2 algorithm (version 2 of sequential uncertainty fitting) was chosen for the optimization of parameter estimation [25]. This algorithm is a method of parameter calibration and uncertainty analysis, which improves the prediction accuracy of the model by identifying the key parameters that significantly affect the model output and using the confidence intervals of these parameters. The SUFI-2 algorithm simultaneously takes into account uncertainties in parameters, model structure, measured data, and driving variables. The algorithm SUFI-2 initiates by assuming a diverse array of values for every calibration parameter. It employs the Latin hypercube curve sampling technique for the parameters and simulates the resulting output variables to ensure that the collected data fall within the 95PPU - the 95% prediction uncertainty [26].

Sensitivity analysis of parameters is essential for calibrating parameter rates through the evaluation of input variables in the model and assessing their impact level. To conduct parameter sensitivity analysis in this research, a regression model was utilized, in which the parameters obtained from Latin hypercube sampling were correlated with the values of the objective function, as outlined in equation (3).

$$g=\alpha+\sum_{i=1}^{m}\beta_i\times b_i \tag{3}$$

When g serves as the target function, the regression equation becomes defined by the coefficients α and β_i, with parameter b_i and the count of parameters

m. To evaluate the parameter sensitivity, a T-test was implemented, indicating that the greater the magnitude of the parameter's absolute value, the higher its sensitivity. Meanwhile, in the process, P-values were utilized to determine the significance level of sensitivity; the nearer the P-value is to zero, the greater the sensitivity's magnitude.

Evaluating the model's applicability using the coefficient of determination R^2 and the Nash-Sutcliffe Efficiency coefficient E_{ns} as evaluation indicators [27]. Due to R^2's emphasis on the evaluating correlation, using only R^2 won't identify systematic errors; E_{ns} focuses on evaluating fit, and using only E_{ns} will result in some simulation errors with smaller values being ignored. Therefore, to improve the applicability of the model in the study area, the above two indicators are used. When $R^2 \geq 0.6$ and $E_{ns} \geq 0.5$ are reached, the model simulation accuracy is significantly acceptable, leading to satisfactory simulation outcomes [28].

The calculation for the Nash-Suttcliffe efficiency coefficient E_{ns} is given by formula (4).

$$E_{ns} = 1 - \frac{\sum_{i=1}^{n}\left(V_{m,i} - V_{s,i}\right)^2}{\sum_{i=1}^{n}\left(V_{m,i} - \bar{V}_m\right)^2} \quad (4)$$

Where V represents the variable, and m and s represent measured and simulated data, respectively. i is the serial number of measured or simulated data. $\bar{V}_m$ is the average of the measured values, n is the number of data points for each variable.

The calculation of the coefficient of determination R^2 is formula (5).

$$R^2 = \frac{\left[\sum_{i=1}^{n}\left(V_{m,i} - \bar{V}_m\right)\left(V_{s,i} - \bar{V}_s\right)\right]^2}{\sum_{i=1}^{n}\left(V_{m,i} - \bar{V}_m\right)^2 \sum_{i=1}^{n}\left(V_{s,i} - \bar{V}_s\right)^2} \quad (5)$$

Results and Discussion

SWAT Model Construction Results

In the SWAT model, the current distribution of land use and soil types can be extracted and reclassified based on basin DEM. The various land use categories within the Guanlan River basin include cultivated land (AGRR: agricultural land row crops, accounting for 0.95% of the area), forest land (FRSE: forest-evergreen, accounting for 20.01% of the area; PEAS: garden or Canning peas, accounting for 1.16% of the area; FRST:

Table 1. Divisions of hydrological response units.

Sub-basin number	Area/km^2	Area proportion /%	Number of HRUs	Average elevation/m
1	3.94	1.53	4	26.64
2	3.91	1.52	2	26.19
3	20.80	8.10	8	61.75
4	24.70	9.62	6	75.04
5	24.83	9.67	10	35.03
6	16.35	6.37	12	99.81
7	15.75	6.14	8	60.97
8	3.30	1.29	8	39.28
9	62.58	24.38	6	63.81
10	36.49	14.21	6	108.45
11	3.41	1.33	4	64.74
12	16.07	6.26	6	103.35
13	24.61	9.59	5	96.41

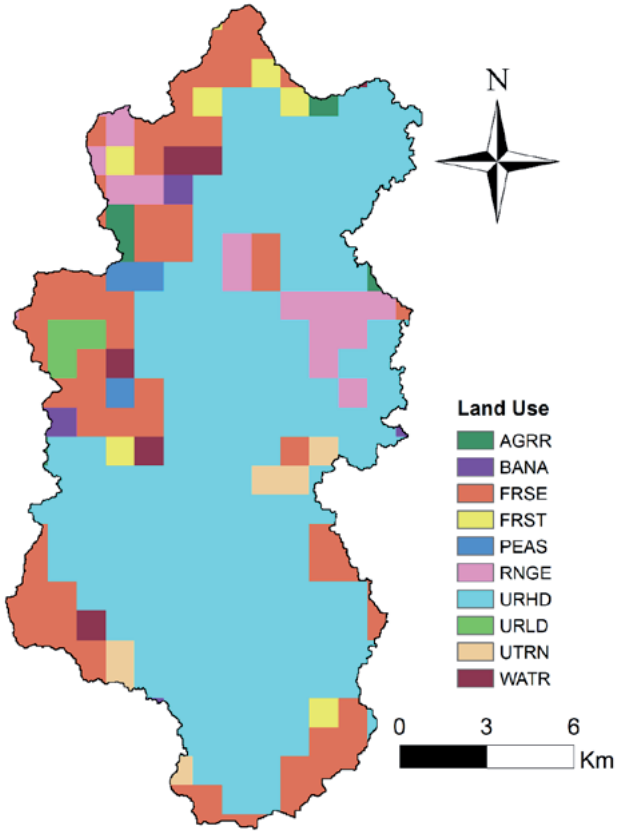

Fig. 2. Land use type distribution in the study area.

forest mixed, accounting for 2.32% of the area; BANA: Bananas, accounting for 0.83% of the area), grassland (RNGE: range grasses, accounting for 5.32% of the area), water (WATR: water, accounting for 1.98% of the area), and urban and rural industrial and mining residential land (URHD: residential-high density, accounting for 64.31% of the area; URLD: residential-low density, accounting for 1.15% of the area; UTRN: Transportation, accounting for 1.98% of the area), with URHD accounting for the most significant proportion, as depicted in Fig. 2.

The soil type includes Gleyic Podzols (accounting for 21.33% of the area), Haplic Podzols (accounting for 6.59% of the area), Haplic Acrisols (accounting for 3.46% of the area), Dystric Cambisols (accounting for 34.37% of the area), Fibric Histosols (accounting for 30.68% of the area), Eutric Cambisols (accounting for 30.68% of the area), Eutric Cambisols (accounting for 3.46% of the area), Haplic Greyzems (accounting for 0.11% of the area), as shown in Fig. 3.

In this study, the SWAT model of the study area is generated based on the 30 m accuracy DEM, which covers an area of 256.72 km^2, and the entire study region has been segmented into 13 distinct sub-basins. This segmentation was achieved by applying a threshold of 1500 ha for the delineation of each sub-basin.

The accuracy and speed of calculation in hydrologic modeling are essential for analyzing watershed behavior. To achieve this, it is important to establish appropriate thresholds for dividing the study area into hydrologic response units (HRUs) based on land use, soil type, and slope. In this study, the thresholds were set at 10% to ensure a relatively reasonable distribution of HRUs within each sub-basin. This approach resulted in the division of the entire study area into 85 HRUs, allowing for a more detailed and accurate representation of the hydrologic characteristics of the watershed. Table 1 illustrates the distribution of HRUs within each sub-basin. All of the HRUs have topographic slopes between 2.76% and 35.82%, with 41 HRUs with slopes between 2.76% and 10%, representing 23% of the area; 30 HRUs with slopes between 10% and 20%, representing 55% of the area; and 14 HRUs with slopes between 20% and 35.82%, representing 22% of the area.

Due to the fact that the SWAT model's default parameter values in the urban database are primarily based on research conducted in urban development areas within the United States, non-point source pollution varies significantly from country to country and region to region [29]. Therefore, when building the SWAT model for analyzing non-point source pollution in high density urban areas, it is essential to adjust the model's parameter values to align with local conditions. Key parameter definitions within the SWAT model's urban module are detailed in the technical reports [30].

The values of FIMP, FCIMP, and CURBDEN are determined based on on-site land use type distribution surveys in the study area, while the values of DIRTMX,

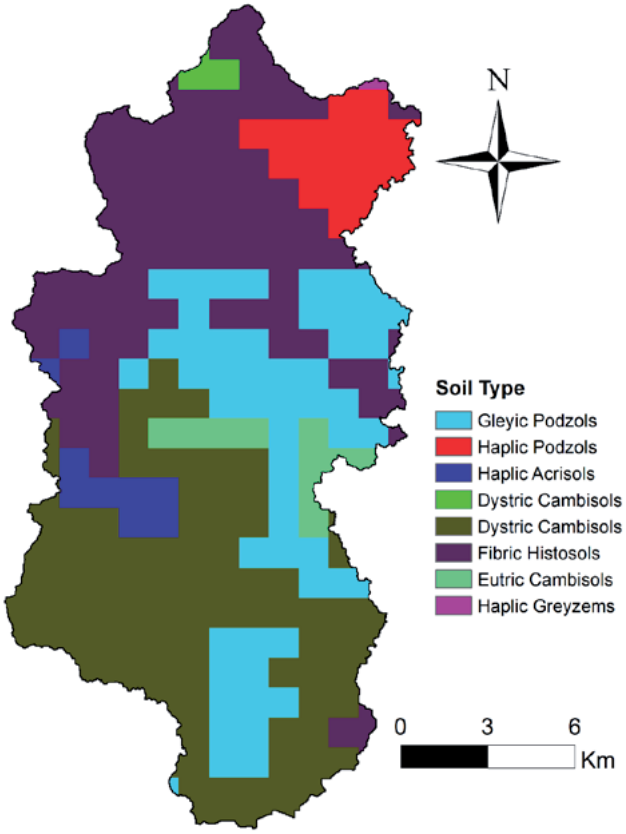

Fig. 3. Soil type distribution in the study area.

TNCONC, TPCONC, and TON3CONC are determined based on surface sediment research. According to the research findings by pertinent scholars [31], the initial parameters in the SWAT model for urban areas of the study area are delineated in Table 2.

URBCOEF, THALF, and URBCN2 were estimated based on the SWAT2009 input-output manual, and CN values were determined based on a previous study in the Guanlan River basin [32].

SWAT Model Calibration and Validation

In this study, water quantity and quality data (TN and TP) were gathered for the discharge points in the study region from 2020 to 2022. Subsequently, the runoff and water quality underwent calibration and validation processes. The simulation intervals were set at monthly intervals.

For this investigation, data on the quantity and quality of water (TN and TP) were Subsequently, the runoff and water quality underwent calibration and validation processes. Monthly simulation intervals were established for the study.

The SUIF-2 algorithm was utilized to conduct parameter sensitivity analysis on the SWAT model parameters, revealing the 15 most significant parameters affecting runoff in the basin, as well as 6 parameters playing a critical role in TN load and 5 parameters significantly affecting TP, as shown in Table 3. For the definition of these parameters, please refer to the technical reports [30]. Among them, the most sensitive parameters influencing runoff simulation are SOL-BD, ALPHA-BNK, CN2, CH_K2, and SOL-AWC; ERORGN, CDN, and SDNCO are served as paramount for total nitrogen sensitivity. ERORGP, P_UPDIS, and PHOSKD are the predominant factors influencing total phosphorus simulation.

The comparison results contrasting simulated and observed monthly runoff values are presented in Fig. 4. The data reveals that the SWAT model excels in replicating monthly surface runoff, with R^2=0.97 and E_{ns}=0.74 in the calibration period and R^2=0.99 and E_{ns}=0.71 in the validation period. The simulated and observed values of TN and TP loads in the study area are generally consistent, as shown in Fig. 5 and Fig. 6. The measured and simulated values of TN load in the calibration period were R^2=0.89, E_{ns}=0.88, and R^2=0.90, E_{ns}=0.80 in the validation period. The TP load during the calibration period is E_{ns}=0.88, E_{ns}=0.85, and R^2=0.84, E_{ns}=0.76 in the validation period. Consequently, the application of the SWAT model for simulating non-point source pollution load in the study area demonstrates both accuracy and rationality, providing a robust foundation for further analysis below. The results are summarized in Table 4.

Table 2. Critical parameters of the urban database of the SWAT model for the study area.

Land use type	FIMP	FCIMP	CURBDEN (km/ha)	URBCOEF (/ mm)	DIRTMX (kg/km)	THALF (d)	TNCONC (g/ kg)	TPCONC (g/ kg)	TNO3CONC (g/kg)	URBCN2
URHD	0.92	0.81	0.34	0.13	10.84	0.75	81.54	0.65	9.17	98
URLD	0.57	0.49	0.30	0.13	21.69	0.75	21.40	0.21	1.79	98
UTRN	0.90	0.90	0.13	0.13	9.37	3.90	38.80	0.34	4.48	98

Characteristics of Spatiotemporal Distribution of Non-Point Source Pollution

The results of the study utilizing the SWAT model highlighted the spatial distribution characteristics of non-point source pollution loads of TN and TP per unit area in the study area for the year 2022. The analysis indicated that the patterns of non-point source pollution loads per unit area for both TN and TP were consistent within the study area, as displayed in Fig. 7 and Fig. 8. Subbasins 4, 5, 6, and 8 exhibited relatively high levels of non-point source pollution load, with TN ranging from 1036.1 to 1523.9 kg/km^2 and TP spanning from 473.5 to 572.9 kg/km^2.

After the HRU definition, only six types of land use are included in the 85 HRUs, and the area proportion of each land type is: FRSE accounts for 18.77%, FRST accounts for 1.26%, PEAS accounts for 0.78%, RNGE accounts for 4.78%, HRHD accounts for 73.24%, and URLD accounts for 1.18%. The contribution ratio of non-point source pollution loads from various types of land use to the total load is shown in Fig. 9 and Fig. 10, with high density residential areas contributing the highest TN and TP loads, accounting for 60.66% and 72.16%, respectively.

From the perspective of load intensity, 73.24% of the HRHD area contributed 60.66% of TN and 72.16% of TP; 18.77% of the FRSE area contributed 17.85% of TN and 12.95% of TP; 4.78% of the RNGE area contributed 17.1% of TN and 11.34% of TP. The above results indicate that the proportion of TN and TP generated by urban land and agricultural and forestry land is different. TP pollution intensity of urban land is more significant than TN, while TN pollution intensity of agricultural and forestry land is more significant than TP.

Defining the contribution ratio divided by the proportion of area as the evaluation indicator of load intensity, it can be concluded that the contribution ratio of TN divided by the area proportion in the urban area is 0.83, which is less than FRSE (0.95) and RNGE (3.58); the contribution ratio of TP in the urban area divided by the area ratio is 0.99, which is between FRSE (0.69) and RNGE (2.37).

Based on the SWAT model, we further estimated the TN and TP pollution loads from non-point sources entering the water bodies of the study area for each month in 2022. The results are shown in Fig. 11. Notably, the variations in pollution loads exhibit a pronounced temporal pattern. The TN and TP loads in the rainy season notably surpass those observed in the dry season, suggesting a significant positive correlation with rainfall patterns. Among the months involved, May experienced the most severe rainfall runoff pollution in the study area, with TN and TP loads reaching 252.47kg/km^2 and 215.91kg/km^2, respectively.

Table 3. Sensitivity parameters of the SWAT model in the Study area.

Variable	Sensitive parameters	T-test value	P value
Parameters sensitive to discharge	SOL_BD	-2.99	0.00
	ALPHA_BNK	-2.16	0.03
	CN2	1.71	0.09
	CH_K2	1.56	0.12
	SOL_AWC	1.53	0.13
	SURLAG	1.32	0.19
	ALPHA_BF	-1.27	0.21
	SLSUBBSN	-1.15	0.25
	OV_N	0.84	0.40
	CH_N2	0.83	0.41
	GW_DELAY	0.49	0.63
	SOL_K	0.39	0.70
	GW_REVAP	0.30	0.77
	ESCO	0.18	0.85
	GWQMN	-0.16	0.87
Parameters sensitive to Total nitrogen	ERORGN	-5.06	0.00
	CDN	-3.13	0.00
	SDNCO	2.05	0.04
	RCN	-1.13	0.26
	NPERCO	0.95	0.34
	N_UPDIS	0.07	0.95
Parameters sensitive to Total phosphorus	ERORGP	-1.85	0.07
	P_UPDIS	-1.51	0.14
	PHOSKD	1.50	0.14
	PSP	1.18	0.24
	PPERCO	0.37	0.71

Non-Point Source Pollution Mitigation Measures

The study area mostly consists of high density residential and impervious areas. In the HRU of this land use type, the filter strips and grassed waterways operation in the SWAT model were used to simulate its mitigation effect on TN and TP.

Filter strips are vegetated strips that intercept surface runoff and filter pollutants. In the SWAT model, the simulation of the filter strip is controlled by three parameters: FITER_RATIO, FILTER_CON, and FILTER_CH [30]. Among them, FITER-RATIO is the key parameter of this operation. Three scenarios with FITER-RATIO equal to 80, 40, and 20 were selected. Taking 2022 as an example, the impact of different filter strip scenarios in the high density residential area on TN and TP mitigation in the study area was simulated.

Grassed waterways are vegetated channels designed to transport surface runoff and trap pollutants and sediments by slowing the flow velocities. The grassed waterways operation in the SWAT model is controlled by five variables: GWATN, GWATSPCON, GWATW, GWATL, GWATS, and GWATD. Among them, GWATW is the key parameter of this operation. Three scenarios with GWATW equal to 2, 4, and 8 were selected. Taking 2022 as an example, the reduction effects of different grassed waterways operations in the high density residential area on TN and TP in the study area were simulated.

The mitigation effects of non-point source TN and TP pollution loads in the study area under various scenarios are compared. As shown in Table 5, both filter strips and grassed waterways operations exhibit substantial efficacy in reducing TN and TP loads from non-point

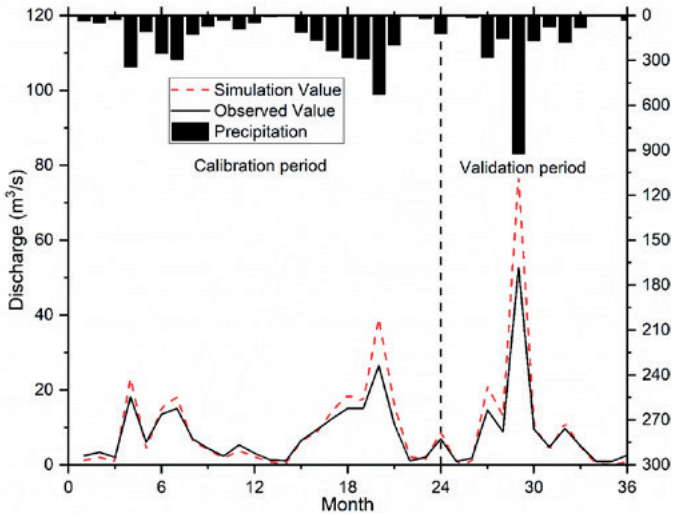

Fig. 4. Simulation of Runoff during the calibration and validation period.

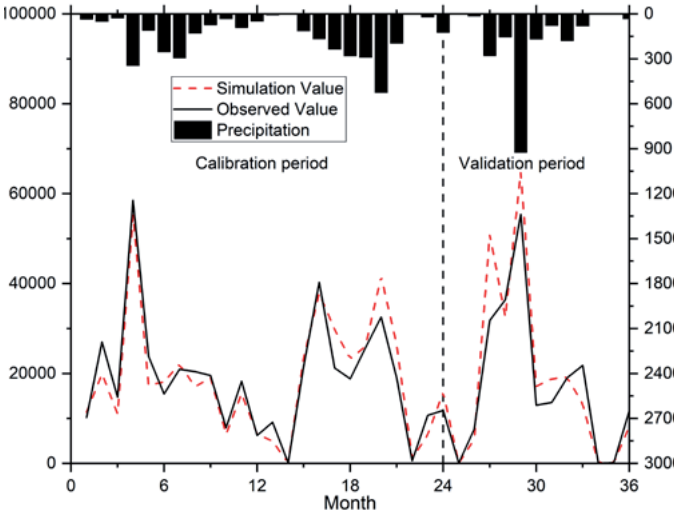

Fig. 5. Simulation of TN load during the calibration and validation periods.

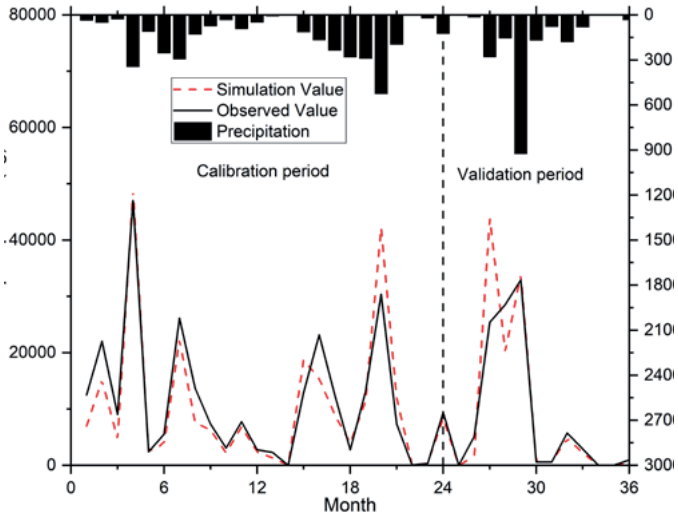

Fig. 6. Simulation of TP load during the calibration and validation period.

Table 4. Evaluating indicator values during the calibration and validation period.

Evaluating Indicator	Evaluation Criterion	Runoff		TN		TP	
		Calibration	Validation	Calibration	Validation	Calibration	Validation
R^2	≥0.6	0.97	0.99	0.89	0.90	0.88	0.84
E_{ns}	≥0.5	0.74	0.71	0.88	0.80	0.85	0.76

Table 5. Reduction effects under different scenarios in high-density residential areas.

Scenarios	TN load		TP load	
	Reduction amount (t/a)	Reduction rate %	Reduction amount (t/a)	Reduction rate %
Filter strips operation (FITER_RATIO = 80)	89.79	38.95	50.52	46.73
Filter strips operation (FITER_RATIO = 40)	96.32	41.78	56.30	52.08
Filter strips operation (FITER_RATIO = 20)	101.58	44.06	59.83	55.34
Grassed waterways operation (GWATW = 2)	6.19	2.68	9.30	8.61
Grassed waterways operation (GWATW = 4)	8.98	3.90	9.42	8.72
Grassed waterways operation (GWATW = 8)	22.69	9.84	10.25	9.48

source pollution, with filter strip operations displaying a more pronounced reduction effect. The reduction effect of filter strip operation on TP is greater than that on TN, particularly as the FITER-RATIO decreases (indicating a larger proportion of filter strips in the area). Yet, the change in reduction rate is relatively modest in comparison to changes in filter strip area, indicating a limitation in the extent to which TN and TP reduction can be enhanced through expanding filter strip coverage.

Considering the operation of the grassed waterway, the reduction rate of TN continuously increases progressively with the increase of GWATW, with the extent of change in the reduction rate amplifying. Conversely, the correlation between its reduction rate of TP and the changes in GWATW is weak, resulting in negligible changes in TP reduction rates across different GWATW scenarios. This indicates that the employment of grassed waterways operation has a restricted capacity to mitigate TP, while increasing GWATW can significantly enhance the reduction of TN.

For basin management aiming at controlling non-point source pollution, particularly in areas characterized by high density residential areas, prioritizing filter strip operation can be determined based on the pollution control objectives of the study area, the existing land use patterns, and the feasibility of implementation. In urban areas where space is limited, the construction of filter strips and ecological restoration of the river channels in the basin can be pursued to establish grassed waterways, further mitigating TN and TP mitigation in non-point source pollution.

Discussion

The SWAT model was utilized in this research to examine the spatiotemporal distribution characteristics of non-point source TN and TP contamination in the study area (high density urban area). Through simulation, the study also assessed the impact of implementing filter strips and grassed waterways on reducing non-point source pollution in urban areas. The findings suggest that these mitigation measures can significantly contribute to improving water quality in high density urban areas by reducing the levels of TN and TP pollution. Implementing such measures is essential for effectively managing and addressing non-point source pollution in urban environments.

From the above simulation results, it can be observed that runoff and non-point source pollution in high density urban areas are significantly and positively correlated with rainfall. This is due to the fact that a large portion of the surface in urban areas is non-permeable, and runoff cannot infiltrate downward into the soil, resulting in insufficient groundwater recharge and the inability to recharge baseflow to rivers during dry periods. On the other hand, surface sediments in

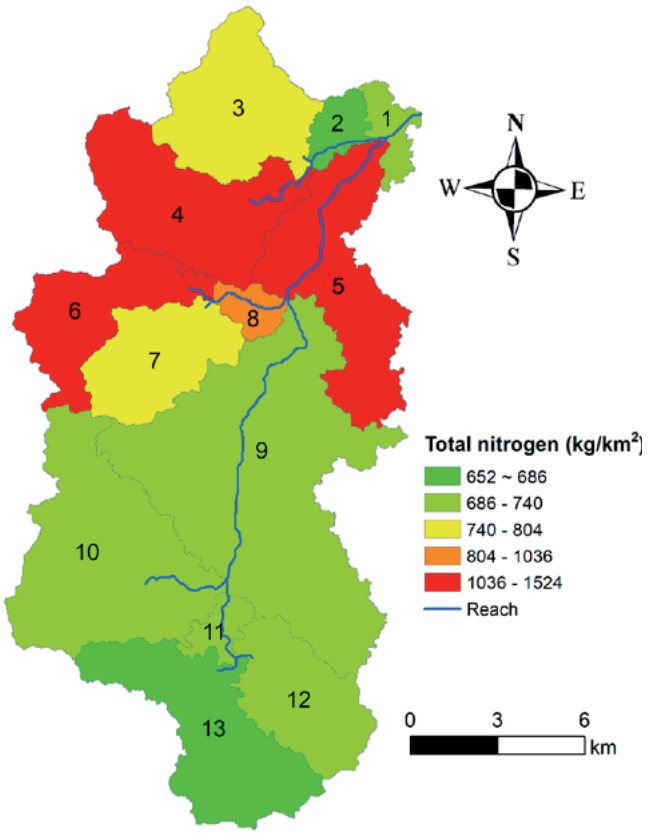

Fig. 7. Spatial distribution of TN output load intensity.

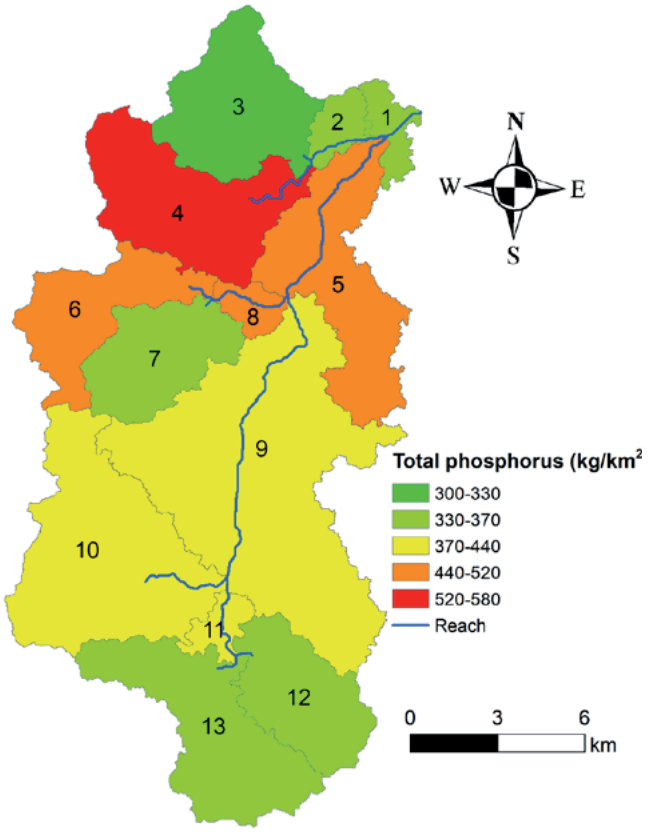

Fig. 8. Spatial distribution of TP output load intensity.

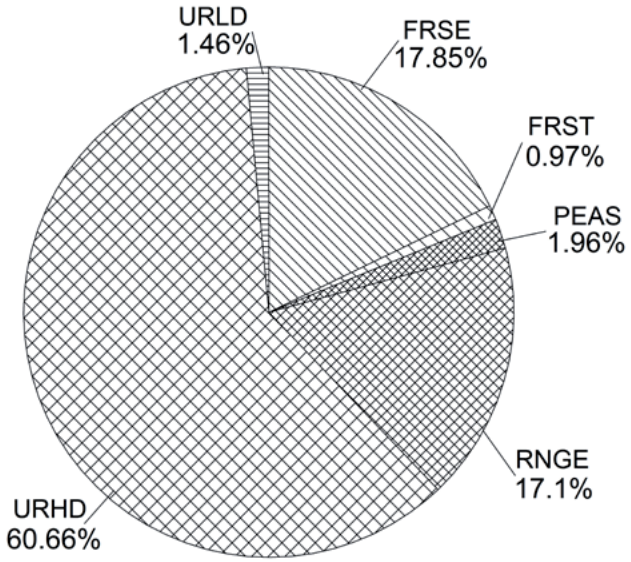

Fig. 9. Contribution ratio of TN for different land use types in 2022.

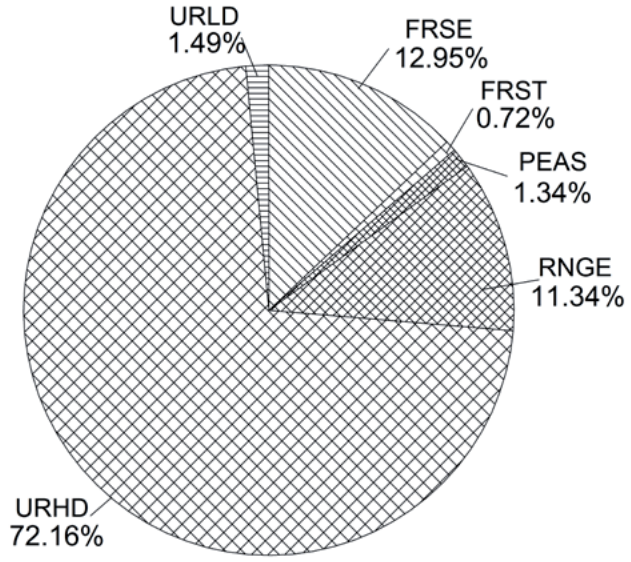

Fig. 10. Contribution ratio of TP for different land use types in 2022.

high density urban areas will remain unchanged after accumulating to a certain amount and will only re-accumulate after rainfall flushing and ground clearing. Moreover, the time to accumulate to the maximum deposition is usually short, so the in-stream loads of TN and TP are positively correlated with the amount and frequency of rainfall.

The factors affecting non-point source pollution in high density urban areas are different from those affecting non-point source pollution in agricultural areas. By analyzing the runoff results from different HRUs in high density urban areas, we found that the runoff generated by HRUs of the same land use type is largely independent of changes in terrain slope. The main reason for this observation is that the SWAT model is calculated on a monthly scale, whereas terrain slope only affects the time of convergence of surface runoff, and the hourly-scale time of convergence has little effect on the monthly-scale runoff output. In addition, there is a correlation between runoff and soil type, mainly because certain areas of urban land are permeable, rainfall runoff can infiltrate through the permeable ground, and surface runoff is smaller when soil permeability is high. In addition, we also compared the calculation results of HRUs for different urban land use types with the same slope and soil type. We found that the main influencing factor is the proportion of impervious area in the urban land type, and as impervious area increases, runoff also increases, mainly due to the decrease in surface runoff from impervious areas, which leads to an increase in overall runoff. TN and TP enter the stream channel through surface runoff, so topographic slope and soil

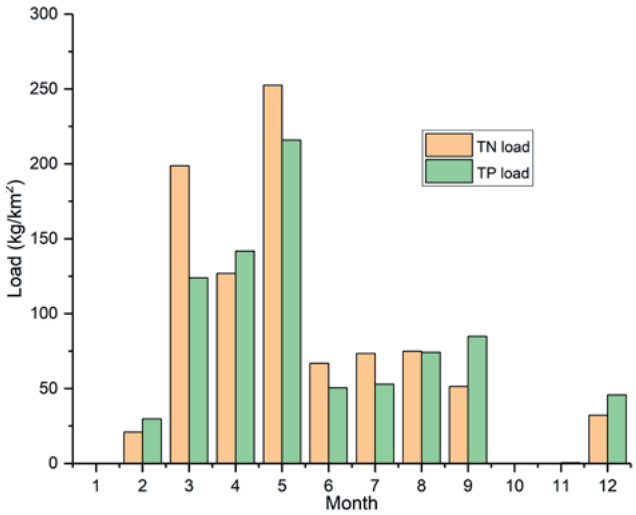

Fig. 11. TN and TP load generated by rainfall runoff pollution in the study area in each month of 2022.

type affect them similarly to runoff. Because TN and TP are derived from surface sediments, the key factor affecting their loading is the concentration of pollutants in the suspended solids from impervious areas.

In order to manage the non-point source pollution in high density urban areas, related scholars have carried out a lot of research, such as using low-impact development measures (rain gardens, vegetated roofs, permeable pavements, etc.) to reduce the non-point source pollution loads, estimating the surface pollution loads in urban areas at a large scale by using remote sensing data [33], or identifying the non-point source pollution sources of the urban areas by using complex methods [34]. Compared with the above methods, the SWAT model in this paper has the advantages of quantitative calculation, high accuracy, and simple evaluation means (without the need to use a lot of complicated sampling and monitoring means) for the assessment of non-point source pollution loads in high density urban areas.

Although this paper has achieved some valuable research results, there are still many shortcomings that require further research. The types of urban land are very complex; in addition to residential areas, there are also industrial land, commercial land, and public management land, and there are apparent differences in their pollution characteristics. The next step is to further refine and study the non-point source pollution load calculation parameters of different land use types in urban areas and to improve the rationality and simulation accuracy of the physical model. In addition, in many high density urban areas, low-impact development measures are currently being used to reduce runoff and pollutant concentrations, so the impacts of these engineering measures on runoff and pollutant concentrations should be considered in the modeling process based on the actual conditions in the study area.

Based on the results of this article, we propose non-point source pollution control methods for high density urban areas from two aspects. Firstly, based on the characterization of spatiotemporal distribution of non-point source pollution, non-point source control plans should be formulated from the aspects of time, zoning, and classification for sub-basins with different land use types; Secondly, low-impact development technologies are adopted to improve the storage, infiltration, and retention of rainwater runoff in high density urban areas during rainfall, and technologies such as filter strips and grassed waterways are used to mitigate the load of pollutants during the transportation process.

Conclusions

In this paper, a SWAT model that can accurately simulate non-point source pollution in high density urban areas is developed through parameter calibration and sensitivity analysis. This study investigated the spatial and temporal loading characteristics of non-point source TN and TP pollution in the study area in 2022. In terms of spatial characteristics, the non-point source pollution load exhibited relatively high pollution loads in sub-basins 4, 5, 6, and 8, with TN ranging from 1036.1 to 1523.9 kg/km^2 and TP ranging from 473.5 to 572.9 kg/km^2. In terms of temporal characteristics, peak rainfall-induced pollution occurred in May, with TN and TP loads reaching 252.47 kg/km^2 and 215.91 kg/km^2, respectively. The TN and TP loads are positively correlated with rainfall and are predominantly influenced by rainwater erosion. Filter strips and grassed waterways proved to be very effective in mitigating non-point source pollution through the modeling analysis. For the six scenarios, TN reductions ranged from 2.68% to 44.06%, and TP reductions ranged from 8.61% to 55.34%. Filter strips showed more significant reductions than lawn waterways.

We considered filter strips and grassed waterways as potential measures to simulate the mitigation effects and characteristics of non-point source TN and TP pollution in the high density urban area of the study area. Filter strip operation indicated a relatively substantial reduction effect as compared to grassed waterways. In managing non-point source pollution in urban areas, prioritizing filter strip operation and, as deemed necessary, integrating grassed waterways operation can lead to further mitigation of TN and TP pollutant concentrations in non-point source pollution. The findings can offer insight for managing non-point source pollution in a similar type of area.

Acknowledgments

There is no acknowledgment in this article.

Conflict of Interest

The authors declare no conflict of interest.

References

1. RONG Q., ZHU S., YUE W., SU M., CAI Y. Predictive simulation and optimal allocation of surface water resources in reservoir basins under climate change. International Soil and Water Conservation Research, **12** (2), 467, **2024**.
2. PASTOR A.V., LUDWIG F., BIEMANS H., HOFF H., KABAT P. Accounting for environmental flow requirements in global water assessments. Hydrology and Earth System Sciences, **18** (12), 5041, **2014**.
3. ZHAO J., ZHANG N., LIU Z., ZHANG Q., SHANG C. SWAT model applications: From hydrological processes to ecosystem services. Science of The Total Environment, **931**, **2024**.
4. LI S., LI J., HAO G., LI Y. Evaluation of Best Management Practices for non-point source pollution based on the SWAT model in the Hanjiang River Basin, China. Water Supply, **21** (8), 4563, **2021**.
5. XIE Z.-J., YE C., LI C.-H., SHI X.-G., SHAO Y., QI W. The global progress on the non-point source pollution research from 2012 to 2021: a bibliometric analysis. Environmental Sciences Europe, **34** (1), **2022**.
6. QU J., WANG H., WANG K., YU G., KE B., YU H.-Q., REN H., ZHENG X., LI J., LI W.-W., GAO S., GONG H. Municipal wastewater treatment in China: Development history and future perspectives. Frontiers of Environmental Science & Engineering, **13** (6), **2019**.
7. ZHANG T., NI J., XIE D. Assessment of the relationship between rural non-point source pollution and economic development in the Three Gorges Reservoir Area. Environmental Science and Pollution Research, **23** (8), 8125, **2016**.
8. AMIN M.G.M., VEITH T.L., COLLICK A.S., KARSTEN H.D., BUDA A.R. Simulating hydrological and non-point source pollution processes in a karst watershed: A variable source area hydrology model evaluation. Agricultural Water Management, **180**, 212, **2017**.
9. AHMADI H. An Overview of Non-Point Source Pollution Modeling: Current Status and Future Prospect. Journal of Civil Engineering Research & Technology, 1, **2023**.
10. DING Y., DONG F., ZHAO J., PENG W., CHEN Q., MA B. Non-Point Source Pollution Simulation and Best Management Practices Analysis Based on Control Units in Northern China. International Journal of Environmental Research and Public Health, **17** (3), **2020**.
11. LIU Y., WANG W., HU Y. Investigating the impact of surface soil moisture assimilation on state and parameter estimation in SWAT model based on the ensemble Kalman filter in upper Huai River basin. Journal of Hydrology and Hydromechanics, **65** (2), 123, **2017**.
12. DUGUMA T.A., WAKIGARI S.A., DILGASA E.A. Analysis of ambo water supply source diversion weir sedimentation and assessing impact of land management practice through hydrological studies. Sustainable Water Resources Management, **6** (6), **2020**.
13. ZETTAM A., BRIAK H., KEBEDE F., OUALLALI A., HALLOUZ F., TALEB A. Efficiencies of best management practices in reducing nitrate pollution of the Sebdou River, a semi-arid Mediterranean agricultural catchment (North Africa). River Research and Applications, **38** (3), 613, **2021**.
14. CHEN H., ZHENG L., WANG W., SHI R. Study on the Effect of Land-Use Change on Phosphorus Pollution In Water China, Jianjiang River, Huazhou Station Control Basin. Polish Journal of Environmental Studies, **31** (3), 2537, **2022**.
15. LIU Y., XING F., ZHOU P., SUN C. Daily-Scale Runoff Simulation of Shanxi Drinking Water Based on SWAT Model, Using Separation Dry and Wet Season Calibration Method. Polish Journal of Environmental Studies, **32** (3), 2221, **2023**.
16. SHEKAR P.R., MATHEW A., S A.P., GOPI V.P. Rainfall-Runoff modelling using SWAT and eight artificial intelligence models in the Murredu Watershed, India. Environmental Monitoring and Assessment, **195** (9), **2023**.
17. TAHMASEBI NASAB M., GRIMM K., BAZRKAR M., ZENG L., SHABANI A., ZHANG X., CHU X. SWAT Modeling of Non-Point Source Pollution in Depression-Dominated Basins under Varying Hydroclimatic Conditions. International Journal of Environmental Research and Public Health, **15** (11), **2018**.
18. LI W., ZHE C., HUI-YING L., DUN-QIU W. Simulation of nitrogen and phosphorus pollution in typical agricultural and forested basins as well as relevant reduction effect based on SWAT model. Water Supply, **21** (3), 992, **2021**.
19. ZEIGER S.J., OWEN M.R., PAVLOWSKY R.T. Simulating non-point source pollutant loading in a karst basin: A SWAT modeling application. Science of The Total Environment, **785**, **2021**.
20. MAO X., HUANG L., HUANG Y., LIU X. Assessment on impacts of Guanlan River comprehensive treatment in Shenzhen City to river health. Water Resources Protection, **31** (1), **2015**.
21. XIE S., LIN H., WANG Y., XU J., CHEN J. Evaluation of Available Rainwater Resources in the Guanlan River Basin of Shenzhen City. Journal of Yangtze River Scientific Research Institute, **39** (7), **2022**.
22. CSEPB Environmental quality standards for surface water (GB 3838-2002). China Environmental Press, Beijing, **2002**.
23. STROKAL M., BAI Z., FRANSSEN W., HOFSTRA N., KOELMANS A.A., LUDWIG F., MA L., VAN PUIJENBROEK P., SPANIER J.E., VERMEULEN L.C.,

VAN VLIET M.T.H., VAN WIJNEN J., KROEZE C. Urbanization: an increasing source of multiple pollutants to rivers in the 21st century. Urban Sustainability, **1** (1), **2021**.
24. ABBASPOUR K.C., VAGHEFI S.A., YANG H., SRINIVASAN R. Global soil, landuse, evapotranspiration, historical and future weather databases for SWAT Applications. Scientific Data, **6** (1), **2019**.
25. MEHAN S., NEUPANE R.P., KUMAR S. Coupling of SUFI 2 and SWAT for Improving the Simulation of Streamflow in an Agricultural Watershed of South Dakota. Hydrology: Current Research, **08** (03), **2017**.
26. ABBASPOUR K.C., JOHNSON C.A., VAN GENUCHTEN M.T. Estimating Uncertain Flow and Transport Parameters Using a Sequential Uncertainty Fitting Procedure. Vadose Zone Journal, **3** (4), 1340, **2004**.
27. GIRI S., NEJADHASHEMI A.P., ZHANG Z., WOZNICKI S.A. Integrating statistical and hydrological models to identify implementation sites for agricultural conservation practices. Environmental Modelling & Software, **72**, 327, **2015**.
28. ZHANG X., CHEN P., DAI S., HAN Y. Analysis of non-point source nitrogen pollution in watersheds based on SWAT model. Ecological Indicators, **138**, **2022**.
29. NEITSCH S.L., ARNOLD J.G., KINIRY J.R., WILLIAMS J.R. Soil and Water Assessment Tool Theoretical Documentation Version 2009. Texas Water Resources Institute, **2011**.
30. ARNOLD J.G., KINIRY J.R., SRINIVASAN R., WILLIAMS J.R., HANEY E.B., NEITSCH S.L. Soil and Water Assessment Tool Input/Output Documentation Version 2012. Texas Water Resources Institute, **2013**.
31. CHEN T., SUN F., YANG S., CHEN L., XIONG X., WANG Y. Load quantification and effect evaluation of urban non-point source pollution in the Guanlan river basin based on SWAT model. Chinese Journal of Environmental Engineering, **14** (10), 2866, **2020**.
32. BAI F., LI T. GIS and L-THIA Based Analysis on Variations of Non-point Pollution in the Guanlan River Watershed, Shenzhen. Environmental Science, **33** (08), 2667, **2012**.
33. HUANG L., HAN X., WANG X., ZHANG Y., YANG J., FENG A., LI J., ZHU N. Coupling with high-resolution remote sensing data to evaluate urban non-point source pollution in Tongzhou, China. Science of The Total Environment, **831**, **2022**.
34. XIONG Q., SONG Y., SHEN J., LIU C., CHAI Y., WANG S., WU X., CHENG C., WU J. Fluorescence fingerprint as an indicator to identify urban non-point sources in urban river during rainfall period. Environmental Research, **245**, **2024**.